EXPERIMENTS WITH A FIXED-BED CATALYTIC REACTOR

SALMA SADDAWI AND ROGER A. SCHMITZ
University of Notre Dame • Notre Dame, IN 46556

In treating the plethora of topics regarding fixed-bed catalytic reactor models, reaction engineering courses typically place emphasis on obtaining basic chemical reaction rate data as a first step. Students learn that expressions for such physical rate processes as fluid dispersion and heat and mass transfer can be formulated and quantified, as a first estimate at least, from various correlations commonly found in handbooks and reaction engineering textbooks. Since an analogous route via correlations is not available for reaction rates, students should understand that obtaining rate expressions and rate constants ordinarily involves experimentation with the particular catalyst and reaction of interest.

The vehicle most recommended for studying catalytic reaction kinetics is the gradientless (completely backmixed or perfectly mixed) reactor in which all physical rate limitations are eliminated, and uniform temperature and pressure conditions are maintained by design and operational procedures. This type of reactor is usually favored over others, such as differential or integral tubular reactors, because conversion in the former is restricted to low levels and nonisothermality and physical rate processes often affect the latter. Well-known types of gradientless reactors are the Carberry spinning basket reactor,[1,2] which is akin to the continuous-flow stirred-tank reactor (CSTR) concept, and the Berty reactor,[3] which is designed for intense internal recycling.

In the laboratory exercise on which this paper is based, senior chemical engineering students at the University of Notre Dame conduct experiments with a small tubular catalytic reactor equipped for an adjustable recycle flow. Their primary objective is to reach a level of recycle where gradientless conditions are evident and, under those conditions, to obtain reaction rate constants. The students are also expected to apply reaction engineering concepts to interpret the observed performance of the reactor without backmixing by recycle flow. The theory and utility of recycle reactors of this type for catalytic reaction studies have been presented in journal articles and in reaction engineering texts.[1,3-9] One of these articles[5] describes the use of such a reactor for studying the kinetics of CO oxidation on supported platinum in an undergraduate laboratory experiment.

The experiments here employ the oxidation of methane on supported palladium. This reaction was chosen mainly because it conveniently serves our purposes. Also, it relates to environmental concerns regarding emissions of unburned hydrocarbons.

As first-semester seniors, students in this laboratory course are taking their first reaction engineering course concurrently. Consequently, depending on the time of the semester, they are not well prepared to appreciate all of the complexities and nuances of fixed-bed reactor models. Therefore the emphasis in this exercise is on the study of the reaction rate under gradientless conditions. Since the students are well grounded in basic transport phenomena from earlier courses, however, their oral discussions, written reports, and analysis of observations can carry the subject beyond idealized reactor models.

In this paper we present our use of data (selected from

Salma Saddawi *is Associate Professional Specialist and Director of Undergraduate Laboratories in Chemical Engineering at the University of Notre Dame. She received her bachelor's degree from Baghdad University and her master's and PhD degrees from Warsaw University of Technology, all in chemical engineering. Her research interests are in catalytic reactions of hydrocarbons, environmental bioengineering, and carbon-carbon composites.*

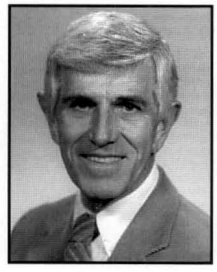

Roger Schmitz *is the Keating-Crawford Professor of Chemical Engineering at the University of Notre Dame. He received his bachelor's degree from the University of Illinois and his PhD from the University of Minnesota, both in chemical engineering. His current interests are in modeling and analysis of environmental and ecosystem dynamics.*

experiments conducted by students in the laboratory course and by a laboratory assistant) to illustrate the type of results that can be obtained and the type of analysis to which those results are amenable.

THE EXPERIMENTAL SETUP

A schematic diagram of the laboratory apparatus is shown in Figure 1. The gaseous feed, a mixture of methane, oxygen, and helium, flows downward through the reactor, which is a 10-mm ID quartz tube of total length 800 mm. (We chose helium as the inert diluent over nitrogen because the latter would obscure an oxygen peak in the gas chromatograph system described below.) The upstream section of the tube, of length 35 cm, serving as a preheat section, is packed with quartz wool and heated by a variable-power heating tape. The reaction zone, 5 cm long, is packed with approximately 1 g (actually 1.0135 g for the data reported here) of cylindrical catalyst pellets of 1/8-inch diameter and length obtained from Engelhard. The pellets are made of alumina support with finely-divided palladium (0.5 wt%) distributed over the pellet surface. The reaction zone is heated by a furnace. Temperatures of both the preheat and the reaction sections are controlled by means of multimode controllers at desired reactor temperatures—which, in the case of sufficiently high recycle flow (the case of the CSTR), is the uniform temperature of the reactor contents. Sensors for the controllers are thermocouples, one located in each section near the outside wall of the quartz tube. Another thermocouple, connected to a digital display, is located at the exit of the catalyst bed. The catalyst bed is supported from below and is held in place by a plug of quartz wool inserted in the downstream end of the reactor tube.

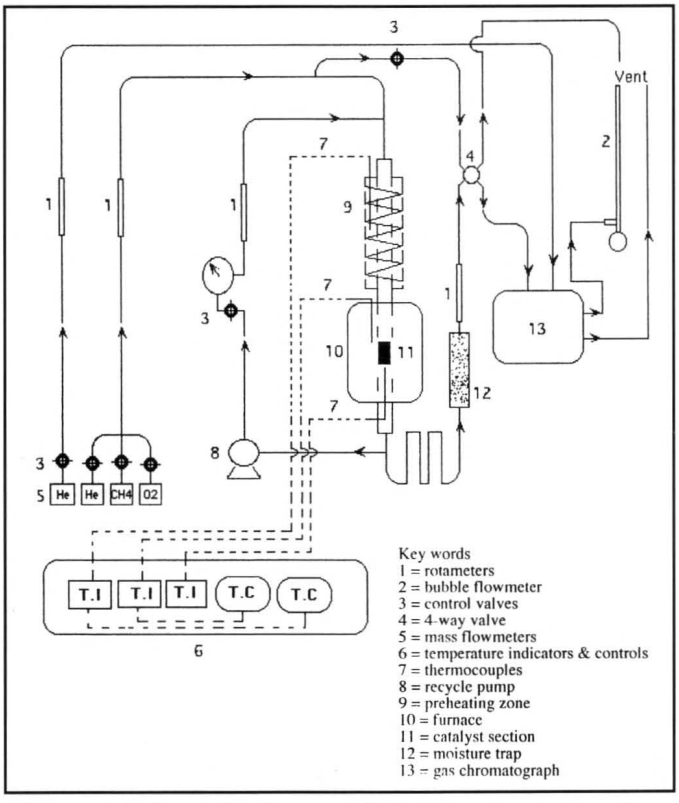

Figure 1. *Schematic diagram of the laboratory apparatus.*

Feed gases are stored in three cylinders, one containing oxygen, another containing helium, and the third containing a mixture of 2% (by volume) methane in helium. Methane is kept in this dilute form for safety purposes, specifically to avoid any possibility that an explosive mixture of methane and oxygen could be inadvertently formed. The lean and rich limits of flammability for methane in pure oxygen are 5.3% and 61%, respectively. The dilute mixture of methane in helium puts all possible feed concentrations safely away from flammability limits.[10]

Nevertheless, we discuss the general concepts of flammability limits with the students prior to their laboratory sessions, and instruct them to adjust the pure helium and oxygen flows first, before injecting the methane-helium mixture. The three feed gases, joined upstream of the reactor, are individually measured and controlled by mass-flow controllers. In addition, the total mixture flow rate is measured by means of a rotameter. In all experiments reported here, the oxygen concentration in the feed was set at 30% by volume, and the helium flow was adjusted so as to achieve the desired methane concentration when combined with a 2% methane-helium mixture.

The recycle flow is forced by a centrifugal compressor in the recycle line and is measured and regulated by means of a rotameter and a valve.

The product stream from the reactor is discharged through the laboratory hood, or alternatively it is directed to an on-line analysis system consisting of a Carle gas chromatograph (equipped with a 6-foot-long Hayesep T 80/100 stainless steel column) and a Hewlett-Packard integrator. With a two-way valve appropriately set, that analysis unit is also used to measure the concentrations in the feed mixture. A number of tests by this method showed that the only reaction product measurable in the dried effluent was carbon dioxide.

This experimental system enables students to investigate parameter effects over relatively wide ranges. Inlet feed concentrations of methane up to 5×10^{-4} mol/liter (at 25°C, 1 atm), reactor temperatures to 350°C, feed flow rates to 0.1 liters/min, and recycle flows to 10 liters/min were feasible. That feed concentration corresponds to a mole percent distribution of 1.2% CH_4, 30.0% O_2, and 68.8% He. All volumetric flow rates and feed concentrations reported here were corrected to 25°C, 1 atm, unless otherwise indicated.

PROCEDURE

Conducting experiments with the system described above amounts to setting the desired flow rates of the individual feed gases, the recycle flowrate, the preheat temperature,

and the furnace temperatures and waiting for steady state to be reached. That state is determined by the temperature measurement at the bed exit and by analysis of the effluent gas stream. The usual procedure for data reported here was to aim for a predetermined effluent temperature by adjusting the furnace and/or preheat temperatures. This necessitated setting the furnace temperature to offset heat losses.

The catalyst itself required no special treatment. It was used as purchased from Engelhard. Its activity remained practically constant for at least one semester.

For the results reported here, the feed flow rate was fixed at 0.1 liters/min, and the methane feed concentration was on the range 1.0×10^{-4} to 4.2×10^{-4} mol/liter (or 0.25% to 1.0% by volume). The reactor temperature covered the range 150°-325°C. The maximum recycle flow was 7.5 liters/min, giving a maximum ratio of recycle to fresh-feed flows of 75.

EXPERIMENTING WITH THE RECYCLE FLOW

In the first stage of experimentation, the students observe the effect of recycle flow, with the specific aim of ascertaining gradientless conditions in the reactor section. Data in Figure 2 show that the effect of recycle flow becomes relatively small above a rate of 2.0 liters/min, and also show a convergence to the curve for 7.5 liters/min over the entire conversion range. Based on this observation, we used a rate of 7.5 liters/min for the kinetic studies reported here and assumed perfect mixing. Discussion in a later section calls attention again to Figure 1 with reference to the data for zero recycle flow.

EQUATIONS FOR A GRADIENTLESS REACTOR

For our purposes, the oxidation of methane is envisioned as a single-step reaction

$$CH_4 + 2\,O_2 \xrightarrow{Pd} CO_2 + 2\,H_2O \qquad (1)$$

with a rate expression of the form

$$r(C,T) = k(T)C^n = k_o\, e^{-\frac{E}{RT}} \left(\frac{T_r}{T}\right)^n C_r^n \qquad (2)$$

where r(C,T) is the rate of methane conversion per mass of catalyst and C_r is the methane concentration corrected to the reference temperature T_r, taken to be 25°C throughout. The correction is based on the assumptions that the gas mixture is ideal and that pressure is constant at 1 atm. All symbols are defined in a table at the end of this paper.

By starting with a rate expression of the form in Eq. (2), we are tacitly sidestepping the mechanistic steps of adsorption and desorption of reactants and products on active sites. Or, stated differently, we are assuming that those steps can be accounted for effectively by an empirically determined value of the reaction order n. Since oxygen is present in large excess and at constant concentration throughout, its effect on the rate is absorbed in k_o.

The starting point for the correlation of data is the following familiar form of the steady-state material balance on a reactant under gradientless conditions

$$r(C,T) = \frac{q_r}{m} C_{or}\, x \qquad (3)$$

where x, the fractional conversion of methane, is given by

$$x = 1 - \frac{C_r}{C_{or}} \qquad (4)$$

Substituting from Eq. (2) for r(C,T) and from Eq. (4) for C_r, casts Eq. (3) in the following form, which relates methane conversion to rate constants and operating conditions

$$\frac{x}{(1-x)^n} = \frac{m}{q_r} C_{or}^{n-1} \left(\frac{T_r}{T}\right)^n k_o\, e^{-\frac{E}{RT}} \qquad (5)$$

We followed the usual procedures of calculating rates from experimental conversion data using Eq. (3) and correlating those rates by way of Eq. (2) to determine values for n, k_o, and E/R. For this purpose we used measured rates of methane conversion at eight temperature levels (between 220° and 290°C). The feed rate, q_r, and the amount of catalyst, m, were not changed in these experiments. Before starting that correlation procedure, we sought an initial indication of the reaction order by constructing the curves, shown in Figure 3, of methane conversion versus concentration in the feed. Regarding that figure, we point out that an analysis of Eq. (5) reveals that the slope of the curves should be negative for n<1, zero for n=1, and positive for n>1. The negative slope of all curves in Figure 3 clearly points to a fractional value for n in our case.

The negative slopes of the curves in Figure 3 could be

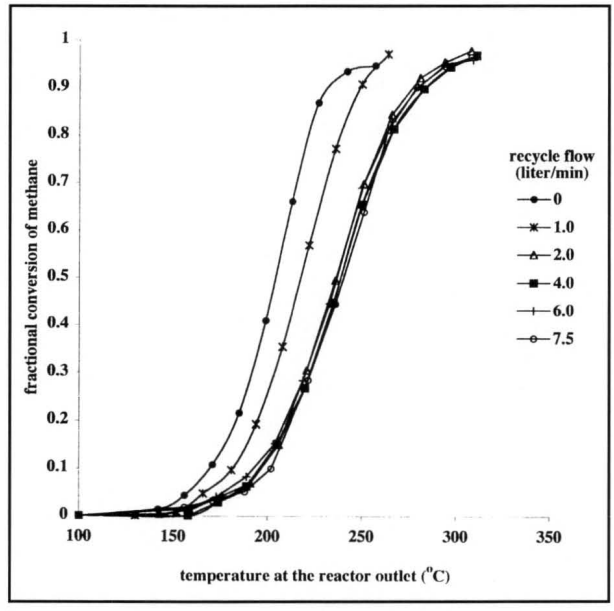

Figure 2. *The effect of recycle flow on methane conversion for a feed concentration, C_{or}, of 1.976×10^{-4} mol/liter.*

explained also in terms of a first-order reaction on active sites with product inhibition. A kinetic study by Ribeiro, *et al.*,[11] supports such a mechanism for methane oxidation on Pd. Earlier studies listed by Culles and Willatt[12] generally reported first-order dependence on methane. Otto[13] correlated data based on a first-order rate, but pointed out that the possibility of half-order, resulting from a possible rate-determining dissociation step, could not be rejected. We have not guided the students toward exploring and testing mechanisms beyond the empirical approach described here, but this is fertile territory for discussion with them as well as for more extensive experimental projects with this apparatus.

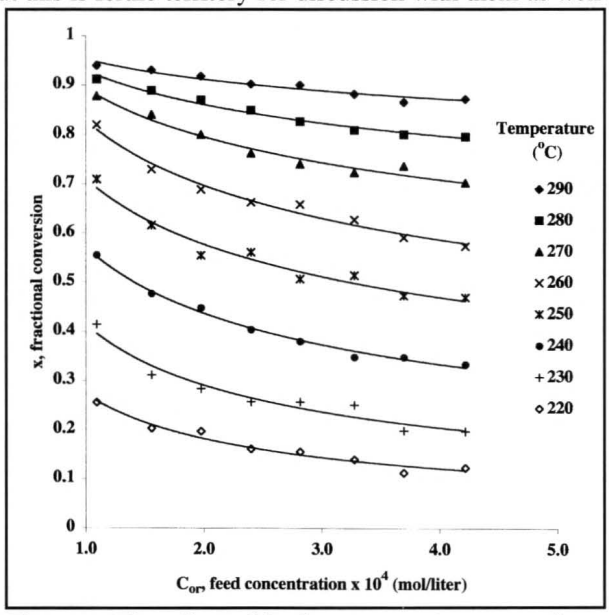

Figure 3. *The effect of feed concentration on methane conversion under gradientless conditions. The curves are least-squares polynomial representations of the data.*

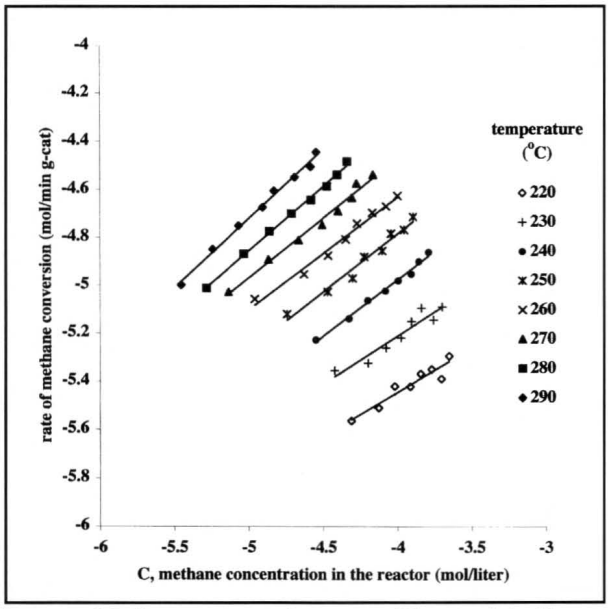

Figure 4. *Methane conversion rates. The straight lines are least-squares representations of the data shown. The numbers on the coordinates are exponents of 10.*

According to Eq. (2), rate data plotted versus C (*i.e.*, $C_r T_r / T$) on logarithmic coordinates should fall on straight lines with slopes equal to the effective reaction order, n, and intercepts equal to k(T)—provided, of course, that our hypothesized rate expression has the appropriate form. As shown in Figure 4, straight lines suitably represent the data over the entire range of conditions of interest here. The values of n, determined from the slopes of these lines, range from 0.37 to 0.58 with an average value of 0.476. Owing to our desire to work with simple rational value, we deemed that an order of one-half was satisfactorily close. Thus, we forced lines with a slope of 0.5 through the data points of Figure 4 and used the corresponding values of k(T), taken from the intercepts, to construct the Arrhenius plot of Figure 5. The following values for k_o and E/R resulted from the least-squares line shown on that plot:

$$k_o = 4.72 \times 10^6 \frac{(\text{mol liter})^{\frac{1}{2}}}{g_{cat}\ \text{min}} \tag{6}$$

$$\frac{E}{R} = 11477°K \tag{7}$$

To put these results to the final test, all of the data are plotted on the coordinates shown in Figure 6. According to Eq. (5), data from experiments as described above should fall on a single curve in the figure, presumably close to the theoretical curve governed by Eq. (5). In short, the good agreement, shown in Figure 6, between observed and predicted results justifies the rate expression in Eq. (2) with n=1/2, and, k_o and E/R given by Eqs. (6) and (7).

Considering the aforementioned fact that certain other investigators used a first-order rate expression, we worked through an alternate approach in which we took n to be unity in Eq. (2) from the start and plotted the rate data for each temperature on linear coordinates versus C. The values of k(T), determined from the slopes of least-squares straight lines on those coordinates, led to an Arrhenius plot where the data appeared to be suitably represented by a straight line—albeit one with greater residuals than those in the Arrhenius plot of Figure 5. The plots of Figures 3 and 4 are persuasive discriminators, even by eyeball judgment, in favor of fractional-order kinetics. Our observations from the alternate approach, however, suggest that rather than systematically changing one variable at a time (the only method we have employed so far), a procedure based on a series of experimental runs statistically designed for model discrimination and parameter estimation might be instructive and interesting.

AN IDEAL PLUG FLOW MODEL

Here, attention is turned to the case of zero recycle, which gives much higher methane conversions experimentally than

the gradientless case shown in Figure 2. Various models can be constructed to represent this case. In one way or another, they might account for axial and radial dispersion, wall heat transfer, and fluid-pellet heat and mass transfer. We present here the simplest model based on assumptions that

- *The reactor temperature is uniform throughout at the effluent temperature (as in the perfect-mixing case)*
- *Mass dispersion, and fluid-pellet mass and heat transfer resistances, are negligible*

Our intent is to consider a model, other than perfect mixing, that students are equipped to analyze and that gives them some basis for discussion of the experimental observations represented in Figure 2. Beyond that, we do not justify the assumptions, which in fact are not valid as we show later. In any case, some of the physical features of the reactor configuration, such as the small ratio of tube diameter to pellet size, uncertain wall heat transfer, and entrance flow effects, make it unlikely that the usual modeling and simulation approaches would be instructive, much less successful, in describing the quantitative behavior of this reactor.

The ideal plug flow isothermal reactor is described by the following differential equation for the methane material balance:

$$\frac{dC}{d\xi} = -\frac{m}{q_r}\frac{T_r}{T}k(T)C^{\frac{1}{2}} \qquad (8)$$

where ξ is the axial position, made dimensionless by the reactor length. The initial condition for Eq. (8) is the concentration at ξ=0.

$$C(0) = C_{or}\frac{T_r}{T} \qquad (9)$$

For the constant temperature case, Eq. (8) is readily integrated to give the concentration as a function of position. Application of Eq. (9) and substitution of the fractional conversion x (now the conversion at ξ=1) from Eq. 4 leads to the following equation for the reactor conversion:

$$x = 1 - \left[1 - \frac{m}{2\,q_r}\left(\frac{1}{C_{or}}\frac{T_r}{T}\right)^{\frac{1}{2}}k(T)\right]^2 \qquad (10)$$

(If the bracketed quantity in Eq. (10) is less than or equal to zero, x should be set equal to unity.)

The reactor conversion predicted by Eq. (10) for C_{or}=1.976x10^{-4} mol/liter, with values of other constants as defined earlier, is shown by the dashed curve of Figure 7. The solid curve in that figure is the conversion for the backmixed reactor calculated from Figure 2 for zero recycle and for a recycle flow of 7.5 liters/min.

The differences between the dashed and solid curves illustrate and reinforce what students find in reaction engineering textbooks—that is, for a positive-order reaction, higher conversions are expected in an isothermal reactor if backmixing does not occur. If a theoretical solution were worked out for intermediate recycle rates, the resulting curves would lie within the envelope formed by the two curves of Figure 7. However, the experimental data points for zero recycle show far greater conversion than that predicted by the models used here—an observation that initiates discussions and analyses along the lines presented in the next section.

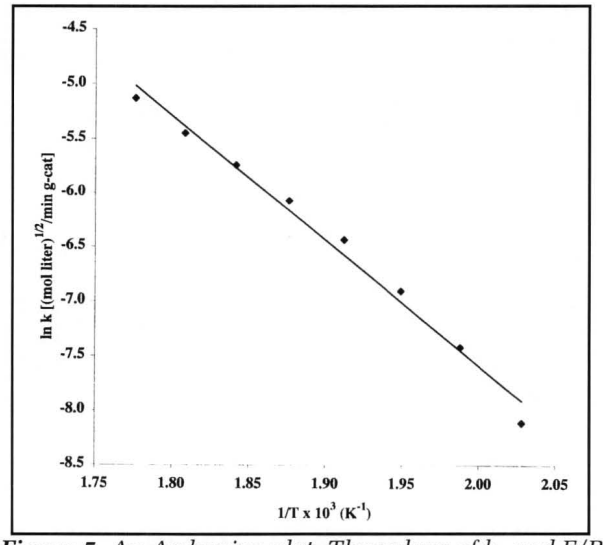

Figure 5. *An Arrhenius plot. The values of k_o and E/R, determined from the least-squares line shown, are given in Eqs. (6) and (7).*

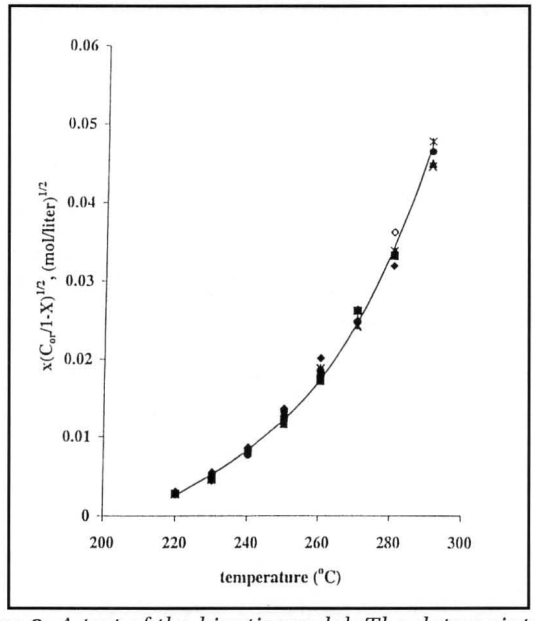

Figure 6. *A test of the kinetic model. The data points are from the set in Figure 3. The curve represents computed values from Eq. (5) for n=1/2 with k_o and E/R given by Eqs. (6) and (7).*

CONSIDERING HETEROGENEITY

It turns out that in order to force the plug flow (dashed) curve of Figure 7 through the experimental data points for zero recycle, the rate constant (k_o) has to be increased by a factor of about five—strong evidence that the catalyst surface is at an appreciably higher temperature than the gas phase. If heat and mass transfer rates are considered, the model must incorporate the following material and energy balances over the fluid-solid interface:

$$Ka(C - C_s) = k(T_s)C_s^{1/2} \tag{11}$$

$$ha(T_s - T) = (-\Delta H)k(T_s)C_s^{1/2} \tag{12}$$

where K and h are mass and heat transfer coefficients, respectively, and the subscript s refers to conditions on the catalyst surface. The two equations can be combined to obtain the following equation relating C_s to T_s:

$$C_s = C - \frac{h}{K}\frac{(T_s - T)}{(-\Delta H)} \tag{13}$$

(If the right side of Eq. (13) is negative, C_s should be set to zero—a mass transfer controlled situation.)

Finally, substitution for C_s from Eq. (13) into Eq. (12) gives the following equation from which the catalyst surface temperature, T_s, can be calculated for a given state T, C in the bulk fluid:

$$ha(T_s - T) = (-\Delta H)k(T_s)\left[C - \frac{h}{K}\frac{(T_s - T)}{(-\Delta H)}\right]^{\frac{1}{2}} \tag{14}$$

Students should realize at this point, or be instructed, that Eqs. (13) and (14) must be coupled to material and energy balances for the bulk fluid—the former possibly being Eq. (8) with subscript s on T and C on the right of the equal sign. A complete simulation exceeds our expectations for this project. Nevertheless some instructive information, both qualitative and quantitative, can be gleaned from further analysis of Eq. (14).

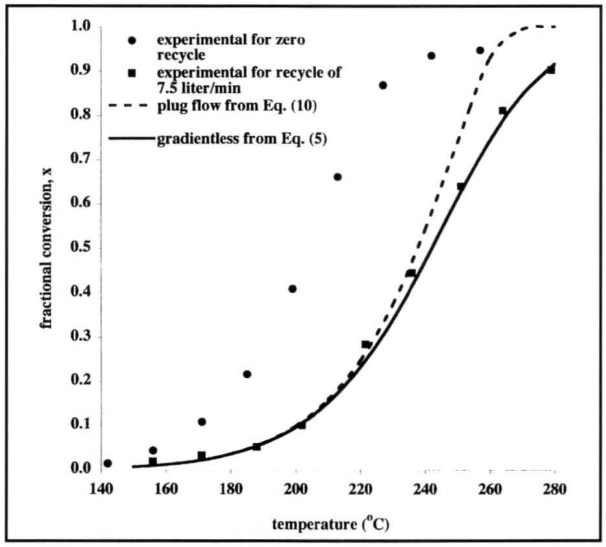

Figure 7. *Comparison of experimental and model-predicted methane conversions.*

By the classic approach,[14,15] the right side of Eq. (14) represents the rate of heat generation by reaction on the catalytic surface and the left side, the rate of heat loss. When plotted versus catalyst temperature, the right side yields a curve of the type shown by the solid curve in Figure 8. The curve first increases, and eventually decreases as reactant mass transfer limits the rate. The left side is a straight line of slope, ha, intersecting the abscissa at T, the bulk temperature.

The dashed lines of Figure 8 show four such cases. The value of the abscissa corresponding to the intersection of the generation and loss curves gives the value of T_s that satisfies Eq. (14). As already mentioned, the curves are dependent on the temperature and concentration, T and C, in the bulk fluid, taken for the illustration in Figure 8 to be 220°C and 1.2×10^{-4} mol/liter, respectively. (The values of constants used in Figure 8 are given in the caption.) The illustration shows that for a sufficiently small value of the coefficient, ha, the catalyst surface temperature can reach a value significantly higher than that of the bulk fluid. In this example, in order to achieve rates five times those at the bulk condition, the catalyst temperature would have to be about 256°C.

This òows that the temperature heterogeneity of the catalyst bed provides an explanation for the high conversions shown by experimental data in Figure 7, but we should add some comments about the magnitudes of the transfer coefficients. The available correlations, such as those for the j-factors,[16] hardly apply in this case—this case being one

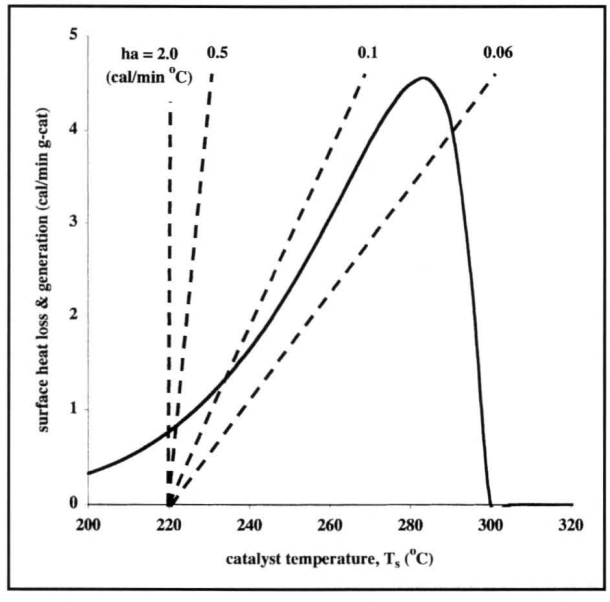

Figure 8. *Heat generation (solid curve) and heat loss (dashed lines) rates from Eq. (14)for four values of the coefficient ha. For these computations, ΔH=191,764 cal/mol; h/K=3x10^{-4} cal/cm^{3}K; C=1.2x10^{-4} mol/liter; T=403 K; k_o and E/R taken from Eqs. (6) and (7).*

that involves a small laboratory reactor containing some 21 catalyst pellets and operating with a Reynolds number of about five or six based on the tube diameter (about three based on pellet size). If forced into use, however, they give a value for ha of about 0.5 cal/min°C and for h/K of about 3×10^{-4} cal/cm^3°C. As the illustration in Figure 8 shows, the difference between the T_s and T for that value of ha is only a few degrees.

Speculating, as we might considering the uncertainty in estimating the appropriate transfer coefficients, that the low Reynolds numbers and relatively large pellets lead to very nonuniform transport rates, the local coefficients could vary over a range as large as that shown for the family of straight lines in Figure 8. If so, catalyst temperatures could exceed the bulk temperature by 60 centigrade degrees or more in some spots. For certain conditions, the curves of Figure 8 could have three intersections, giving rise to multiple states of the type studied by Liu and Amundson[14] and Liu, *et al.*[15] We have seen no evidence of such multiplicity in laboratory experiments to date.

Since the present experimental system is not equipped with a means of measuring local catalyst temperatures, our analysis of the zero-recycle case reaches its conclusion at this stage. Incidentally, the aforementioned correlations, when used for the earlier "gradientless" case where the recycle rate was 7.5 liters/min, give a value for ha of about 2.0—the value corresponding to the nearly vertical line in Figure 8. Students can now appreciate the fact that increasing the recycle flow in the experiments illustrated in Figure 2 causes the slope of the straight line to increase toward infinity, thereby practically eliminating the transport resistances and bringing the fluid and catalyst temperatures together.

CONCLUSION

We have demonstrated the use of a small fixed-bed reactor, equipped for recycle flow, for an undergraduate laboratory experiment. The recycle feature enables students to achieve a gradientless condition for rate studies of the oxidation of methane on Pd-coated catalyst pellets. With zero recycle, heterogeneous effects (especially transport resistances between the fluid and catalytic phases) are important. While full-fledged reactor modeling and simulation accounting for heterogeneity are not attempted for this system, we show how those effects can be analyzed and the reactor performance explained, at least in a pseudo-quantitative manner.

For undergraduate students, this laboratory experience, coupled with the application of the theory described here, is a beneficial complement to the textbook material covered in their reaction engineering course.

NOMENCLATURE

- a External catalyst area per unit mass of catalyst
- cat Subscript used to refer to the catalyst
- C Methane concentration in the bulk fluid
- C_{or} Methane concentration in the feed, corrected to temperature T_r
- C_r Methane concentration in the bulk fluid, corrected to temperature T_r
- C_s Methane concentration at the fluid-catalyst interface
- E Activation energy
- h Coefficient for heat transfer between the bulk fluid and the catalyst surface
- k Reaction rate constant
- k_o Pre-exponential factor in reaction rate expression
- K Coefficient for mass transfer between the bulk fluid and the catalyst surface
- m Mass of catalyst in the reactor
- n Reaction order
- q_r Gas volumetric flow rate corrected to temperature T_r
- r Reaction rate per unit mass of catalyst
- R Universal gas constant
- T Absolute temperature
- T_r Reference temperature (298°K)
- T_s Absolute temperature at the fluid-catalyst interface
- x Methane conversion defined in Eq. 4
- ΔH Enthalpy of the reaction in Eq. 1
- ξ Dimensionless axial position, distance from the inlet divided by reactor length

REFERENCES

1. Carberry, J.J., "Designing Laboratory Catalytic Reactors," *Ind. Eng. Chem.*, **56**, 39 (1964)
2. Tajbl, D.G., J.B. Simons, and J.J. Carberry, "Heterogenous Catalysis in a Continuous Stirred-Tank Reactor," *Ind. Eng. Chem. Fund.*, **5**, 171 (1966)
3. Berty, J.M., "Testing Commercial Catalysis in Recycle Reactors," *Catal. Rev. Sci. Eng.*, **20**, 75 (1979)
4. Weekman Jr., V.W., "Laboratory Reactors and their Limitations," *AIChE J.*, **20**, 833 (1974)
5. Paspek, S.C., A. Varma, and J.J. Carberry, "Utilization of the Recycle Reactor in Determining Kinetics of Gas-Solid Catalytic Reactions," *Chem. Eng. Ed.*, **14**, 78 (1980)
6. Wedel, S., and J. Villadsen, "Falsification of Kinetic Parameters by Incorrect Treatment of Recirculation Reactor Data," *Chem. Eng. Sci.*, **38**, 1,346 (1983)
7. Broucek, R., "Falsification of Kinetic Parameters by Incorrect Treatment of Recirculation Reactor Data," *Chem. Eng. Sci.*, **38**, 1349 (1983)
8. Hidajat, K., F.J. Aracil, J.J. Carberry, and C.N. Kenney, "Laboratory Catalytic Studies: The Role of Transport Phenomena," *J. Catalysis*, **105**, 245 (1987)
9. Levenspiel, O., *Chemical Reaction Engineering*, 3rd. ed., John Wiley & Sons, New York, NY (1999)
10. Lewis, B., and G. von Elbe, *Combustion, Flames and Explosions of Gases*, 2nd ed., Academic Press Inc., New York, NY (1961)
11. Ribeiro, F.H., M. Chow, and R.A. Dalla Betta, "Kinetics of the Complete Oxidation of Methane over Supported Palladium Catalysts," *J. Catal.*, **146**, 537 (1994)
12. Cullis, C.F., and B.M. Willat, "Oxidation of Methane over Supported Precious Metal Catalysts," *J. Catal.*, **83**, 267 (1983)
13. Otto, K., Methane Oxidation over Pt on g-Alumina: Kinetics and Structure Sensitivity," *Langmuir*, **5**, 1364 (1989)
14. Liu, S.L., and N.R. Amundson, "Stability of Adiabatic Packed-Bed Reactors: An Elementary Treatment," *Ind. Eng. Chem. Fund.*, **1**, 200 (1962)
15. Liu, S.L., R. Aris, and N.R. Amundson, "Stability of Nonadiabatic Packed-Bed Reactors: An Elementary Treatment," *Ind. Eng. Chem. Fund.*, **2**, 12 (1963)
16. Froment, G.F., and K.B. Bischoff, *Chemical Reactor Analysis and Design*, John Wiley & Sons, New York, NY (1979)❐